

*Book can be  
File 6-10*

# WORK FUNCTIONS AND CONDUCTIVITY OF OXIDE-COATED CATHODES

G. W. MAHLMAN

TECHNICAL REPORT NO. 67

MAY 31, 1948

RESEARCH LABORATORY OF ELECTRONICS  
MASSACHUSETTS INSTITUTE OF TECHNOLOGY

The research reported in this document was made possible through support extended the Massachusetts Institute of Technology, Research Laboratory of Electronics, jointly by the Army Signal Corps, the Navy Department (Office of Naval Research), and the Air Force (Air Materiel Command), under the Signal Corps Contract No. W-36-039 sc-32037.

MASSACHUSETTS INSTITUTE OF TECHNOLOGY  
Research Laboratory of Electronics

Technical Report No. 67

May 31, 1948

WORK FUNCTIONS AND CONDUCTIVITY OF OXIDE-COATED CATHODES\*

G. W. Mahlman

Abstract

The thermionic and photoelectric work functions and the temperature variation of coating conductivity have been measured for an oxide cathode. Thermionic and photoelectric currents were measured in both retarding and accelerating fields. The two work functions are found to be different, but not by the amount predicted by applying simple semi-conductor theory to the data. Photoelectric currents fit a Fowler plot rather well over a limited range of frequencies. The large decrease in work function with applied field, the poor "saturation" of thermionic currents typical of oxide cathodes, and the behavior of the photoelectric currents in accelerating fields all suggest that one is dealing with a "patchy" surface. Applying "checkerboard" patch theory to the experimental data, one finds that most of the data is accounted for by assuming patches about  $3 \times 10^{-4}$  cm on a side differing in work function by about .2 volt.

---

\* This report is a condensed version of a thesis with the same title submitted by the author in partial fulfillment of the requirements for the degree of Doctor of Philosophy in Physics at the Massachusetts Institute of Technology, 1948.



# WORK FUNCTIONS AND CONDUCTIVITY OF OXIDE-COATED CATHODES

## 1. Introduction

The oxide-coated cathode has many characteristics similar to those of an "excess" impurity semi-conductor. By measurements of the thermionic work function  $\phi_{th}$ , the photoelectric work function  $\phi_{p.e.}$ , and the variation with temperature of the coating conductivity  $\sigma$ , one should be able to learn something concerning energy differences between occupied and unoccupied energy levels in the oxide-coated cathode.

In Fig. 1 is shown a model of the oxide-coated cathode which, it is believed, incorporates most of the elements influencing the electron emission from these cathodes. These elements will be considered separately from left to right.

The base metal usually employed, and the one employed in these experiments, is nickel. No nickel, however, is absolutely pure; even the purest electrolytic nickels contain traces of other metals. These other metals frequently react with the carbonates, oxides, or possibly with the binder, to form a compound between the base metal and the oxide coating referred to as the "interface".<sup>1,2,3</sup> Since the properties of the interface, such as its electrical conductivity, may differ from the other elements, the interface may influence emission from the cathode.

The coating is considered to be an "excess" electronic semi-conductor. The levels in the interior of the BaSrO crystals indicated by the symbol  $\bullet$  in Fig. 1 represent extra electron levels contributed by barium atoms dispersed interstitially through the crystal lattices. These "impurity levels" are electrons unable to move through the lattice until excited into the conduction band.

Fowler<sup>4</sup> derives by statistical theory the following equation for the thermionic emission from semi-conductors:

$$J = \frac{(2\pi mk^5)^{\frac{1}{4}}}{h^{\frac{3}{2}}} D n_p^{\frac{1}{2}} T^{\frac{5}{4}} \exp \left[ \epsilon (-V - \frac{1}{2}E) / kT \right] = A' T^{\frac{5}{4}} \exp(-\epsilon \phi_{th} / kT)$$

$$\text{or} \quad J = 10^{-6} D n_p^{\frac{1}{2}} T^{\frac{5}{4}} \exp \left[ \epsilon (-V - \frac{1}{2}E) / kT \right] \text{ amp/cm}^2 \quad (1)$$

so that  $\phi_{th} = V + E/2$ .  $D$  is the transmission coefficient,  $m$  is electronic mass,  $n_p$  is the number of impurity levels per  $\text{cm}^3$ ,  $\epsilon$  is the electronic

charge,  $k$  is Boltzmann's constant,  $h$  is Planck's constant,  $T$  is the absolute temperature, and  $V$  and  $E$  are the energy gaps indicated in Fig. 1, expressed in volts.

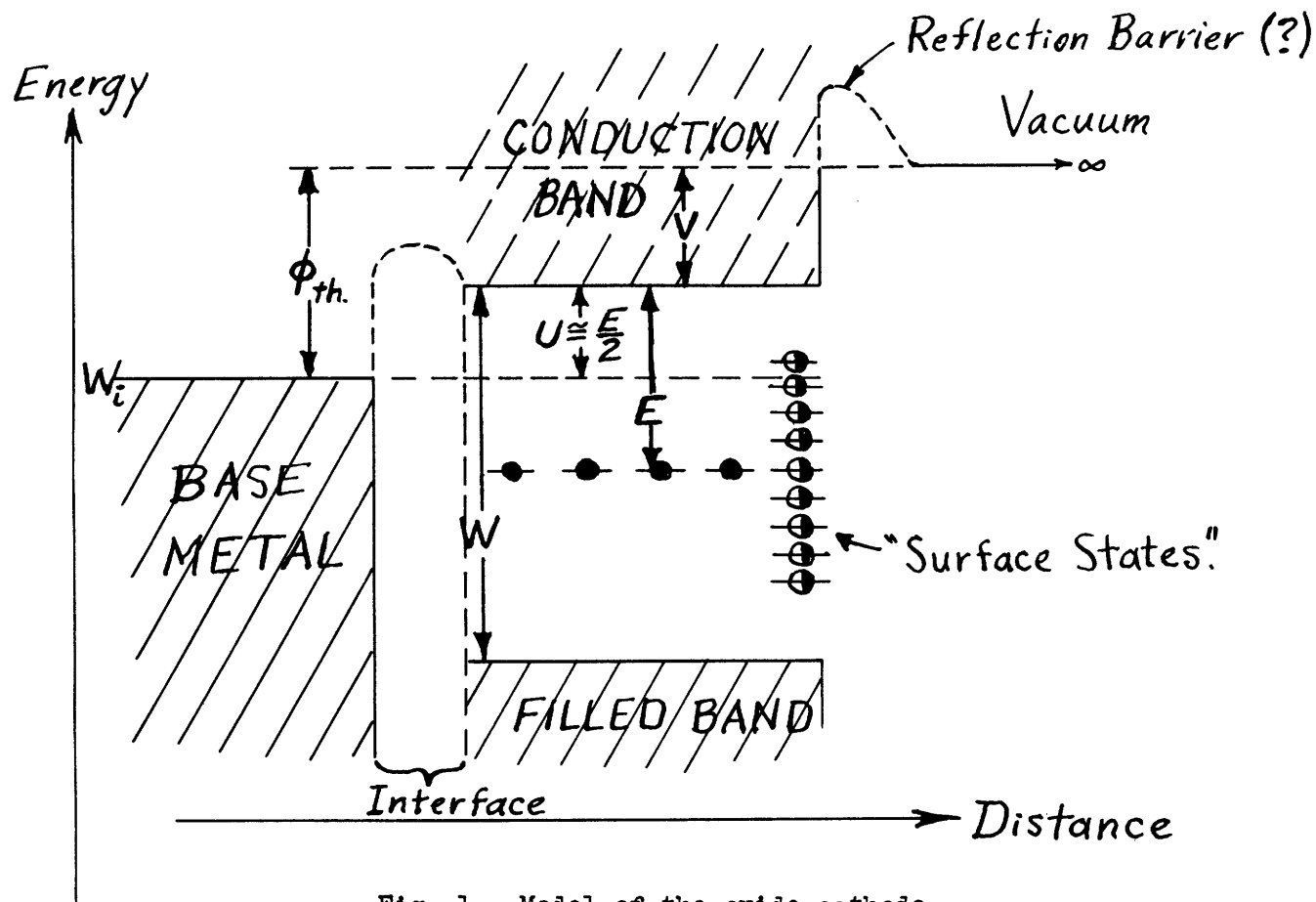


Fig. 1. Model of the oxide cathode.

If we assume that the "surface states" are distributed in the same way as are those in the oxide interior, namely at the impurity levels, by far the greater part of the photoelectrons will come from these levels at room temperature. This means that  $\phi_{P.E.} = V + E$  which is different from  $\phi_{th}$  by the amount  $E/2$ .

The variation of conductivity with temperature is given by the theoretical formula:<sup>5</sup>

$$\sigma = n_b^{\frac{1}{2}} \frac{4\sqrt{2}}{3} \frac{e^2 l_0}{h^{\frac{1}{2}}} (2\pi m^* kT)^{\frac{1}{4}} \exp(-eE/2kT)$$

or

$$\sigma = 0.024 l_0 n_b^{\frac{1}{2}} T^{\frac{1}{4}} \exp(-eE/2kT) \text{ mho/cm} \quad (2)$$

where  $\lambda_0$  is the mean free path, and  $m^*$  is an "effective" electronic mass which may be assumed approximately equal to  $m$ , the true electronic mass. Hence the slope of a plot of  $\log \sigma$  vs.  $1/T$  should be approximately equal to  $-\epsilon E/2k$ . Such a plot gives an experimental determination of the energy gap  $E$ . Experimental determinations of  $\phi_{th}$  and  $\phi_{p.E.}$  permit one to check experimentally the relationships:

$$\left. \begin{aligned} \phi_{th} &= V + E/2 \\ \phi_{p.E.} &= V + E \\ \frac{k}{\epsilon} \cdot \frac{d(\log \sigma)}{d(1/T)} &\cong -E/2 \end{aligned} \right\} \quad (3)$$

"Surface states" may exist, and represent a distribution of electrons in energy different from that in the interior of the crystals. This different distribution of allowed energies could arise from an interruption of the periodicity of the lattice potential at the boundary of the lattice, ("Tamm states") and also from the probable existence of barium on the oxide surface. These states may play a part in emission, particularly surface effects such as the external photoelectric effect.

Some kind of surface potential barrier may exist between the oxide coating and the vacuum outside. This barrier and/or a like barrier at the base metal-coating interface could result in reflection of electrons trying to escape from the cathode. Low-energy electrons might be reflected back into the cathode rather than emitted. If the barrier is only a few Angstrom units thick, electrons have a certain probability of penetrating it by virtue of the quantum-mechanical "tunnel effect". This would lead to a deficiency of slow electrons in a Maxwell-Boltzmann distribution of velocities.

## 2. Experimental Procedure

In these experiments, it is desired to measure the photoelectric work function  $\phi_{p.E.}$ , the thermionic work function  $\phi_{th}$ , and the coating conductivity  $\sigma$  for the same oxide-coated cathode. The currents to be measured are small, so that leakage between electrodes must be minimized. A cross section of the electrode structure of the experimental tube is shown in Fig. 2. The collector and guard cylinders are each  $\frac{1}{2}$  inch in diameter and 10 mm long. The collector has a rectangular window 2 mm x 4 mm, so that

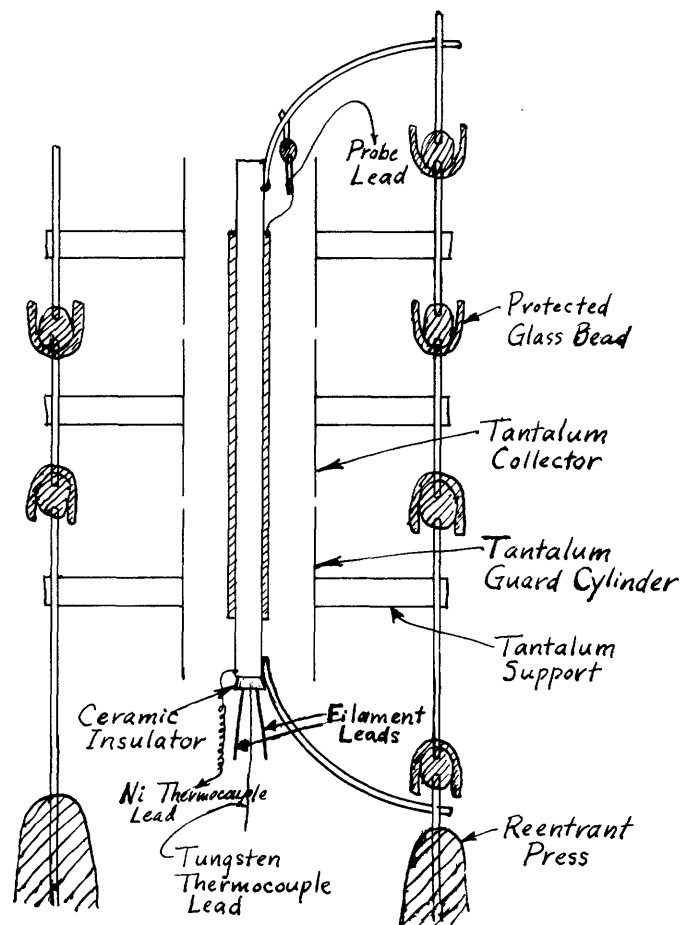


Fig. 2. Cross section of electrode structure.

the oxide cathode can be illuminated. The cylinders are insulated from one another and from the cathode by glass beads. These beads have an outer sheath, open at one end, so that any material emanating from the cathode is deposited on the sheath. This minimizes leakage, which often is serious in tubes having oxide cathodes.

Oxide cathodes having standard commercial nickels as a base metal form interface compounds in many cases. Such interfaces complicate the physical structure with which we are dealing. Indeed, if we are to make a reasonably reliable measurement of  $\sigma$ , it is necessary that the interface conductivity be taken into account. It is thought that the best procedure is to try to eliminate the interface compounds by the employment as a base metal of a very pure electrolytic nickel, designated as Wise No. 1.\* The work of Fineman and Eisenstein,<sup>1</sup> of Mutter,<sup>2</sup> and of Vick<sup>3</sup> indicates that interfaces form on such a nickel only very slowly as the cathode is "aged".

---

\* Procured from E. M. Wise of International Nickel Company.



Coating conductivity is determined by means of a fine ( $\frac{1}{2}$ -mil) platinum "probe" wire embedded in the coating. A coating is sprayed on the nickel sleeve, and the probe wire is spiralled over the length of the coated portion. A second coating is sprayed on to hold the probe wire in place within the coating.

It is believed that the best method of measuring oxide temperature is that employed by Fan.<sup>6</sup> A fine (2-mil) thermocouple wire of tungsten is welded internally to the center section of the cylindrical cathode sleeve. Thus one has a nickel-tungsten thermocouple with which to measure the base metal temperature. It is calibrated by heating such a thermocouple together with an iron-constantan thermocouple in an oven up to about 600°C. This temperature range covers most of the temperatures of interest. Probable error is about  $\pm 10$  degrees. The largest uncertainty in measuring oxide temperature by base metal temperature is the temperature drop through the coating. Probe tube coatings are rather thick (0.025 cm in this case), and Blewett<sup>7</sup> believes temperature drops of 100 degrees or more could take place through the oxide coating. On the other hand, Moore and Allison<sup>8</sup> conclude from their measurements that large temperature drops through oxide coatings are unlikely. Calculations using data in Blewett's article indicate that large temperature drops are particularly unlikely at temperatures less than 900°K. The thermal emf observed between the probe and the base metal is about 16 millivolts at 900°K., and drops rapidly as the temperature of the cathode decreases. The simple theory for the Seebeck emf of a metal-semiconductor contact<sup>4</sup> gives for this emf a value  $\frac{1}{2}E/T$ . The  $\frac{1}{2}E$  determined experimentally is 1.2 volts, so that the Seebeck emf at 900°K. would be approximately 1.3 millivolts per degree, and even higher at lower temperatures. Thus 16 millivolts emf indicates a temperature difference of about 12° between base metal and probe, or roughly twice this through the coating. Excluding some conductivity measurements, all data were taken at temperatures less than 900°K. where all evidence indicates that temperature drops through the coating are less than at 900°K. It is believed that the oxide-surface temperature is known to within about 20 degrees for temperatures up to about 900°K.

In Fig. 3 is indicated schematically the circuits and equipment used to make the various measurements. To obtain monochromatic radiation, the light from a T-10 projection lamp is sent through a single glass monochromator, and focussed on the oxide cathode by a simple lens. The calibration of intensity was accomplished by a thermopile whose approximate sensitivity was 1 microvolt per 2 microwatts illumination. Currents were measured down to about  $10^{-14}$  ampere by a Victoreen VX-41 electrometer tube. Potentials marked "P" in Fig. 3, as well as the thermocouple emf, were determined by a Type K potentiometer.

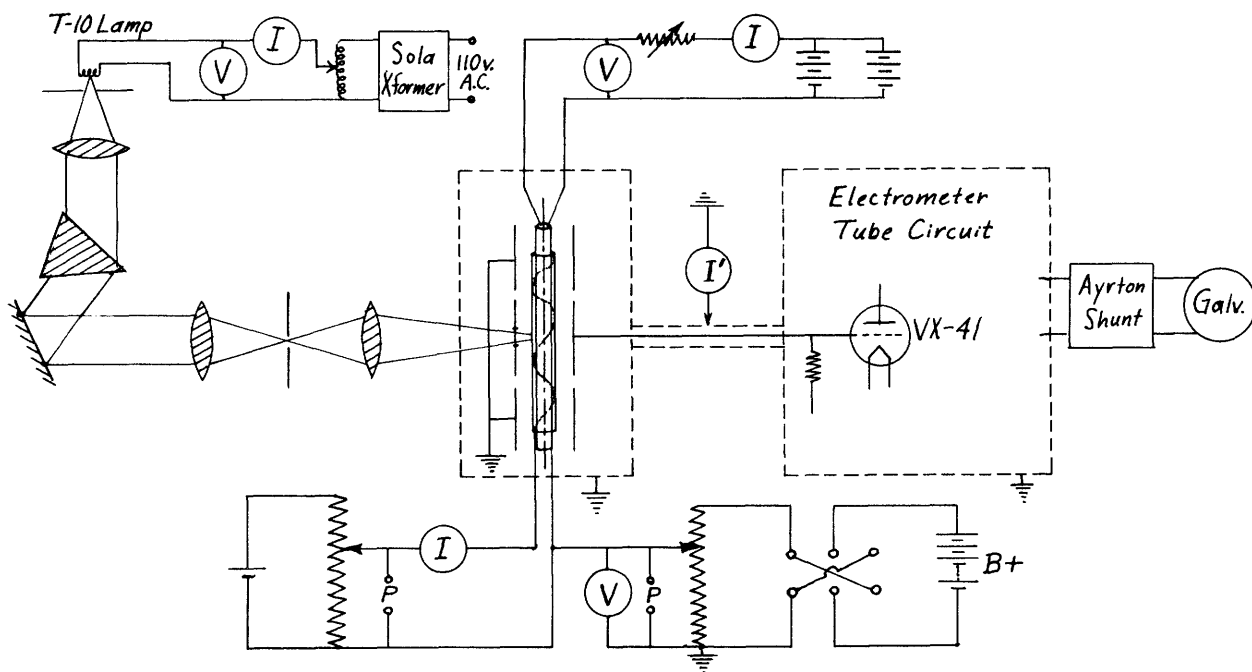


Fig. 3. Experimental circuits and equipment.

### 3. Experimental Results

3.1. Thermionic Emission in Retarding Fields. For a concentric-cylinder geometry, Schottky derived the following equation for thermionic emission in retarding fields, assuming a Maxwellian distribution of velocities:

$$\begin{aligned}
 I = 2I_0/\sqrt{\pi} \left\{ \left[ \exp(-\epsilon V'/kT) \int_0^{\sqrt{\rho \epsilon V'/kT}} \exp \left[ -r^2 \epsilon V'/R^2 kT \right] d \left[ \left( \frac{\epsilon V'}{kT} \right)^{\frac{1}{2}} \right] \right. \right. \\
 \left. \left. + \int_{\sqrt{\rho \epsilon V'/kT}}^{\infty} \exp(-\epsilon V'/kT) d \left[ \left( \frac{\epsilon V'}{kT} \right)^{\frac{1}{2}} \right] \right\} \quad (4)
 \end{aligned}$$

where  $R$  = anode (collector) radius  
 $r$  = cathode radius  
 $\rho = R^2/R^2 - r^2$   
 $V'$  = true retarding potential  
 $I_0$  = current at zero field ("saturation" current).

For plane-parallel geometry  $r \rightarrow R$ ,  $\rho \rightarrow \infty$  and Eq. (4) becomes:

$$I = I_0 \exp(-eV'/kT). \quad (5)$$

The ratio  $R/r$  is small (about 3.4) for the geometry used, so that the theoretical curve ( $\log I$  vs.  $V'/T$ ) has a slope rapidly approaching  $-e/k$  as the retarding field increases from zero, and a fairly sharp "break" at zero field.

Figure 4 shows some of the data taken in the retarding field region. The experimental curves approach the slope  $-e/k$  only for retarding

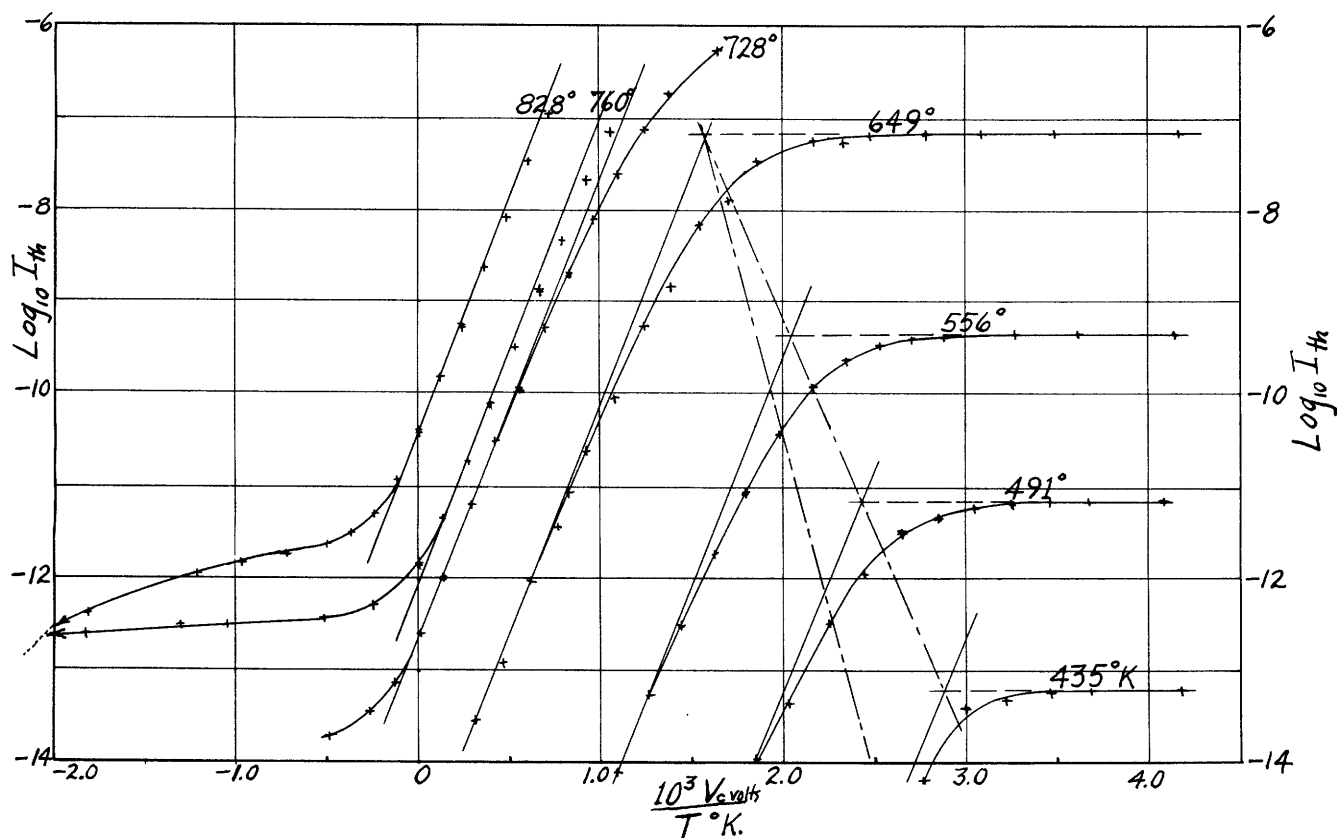


Fig. 4. Retarding potential plots.

fields of several tenths of a volt. It is perhaps significant that the observed curves for the temperatures 649°K., 556°K., and 491°K. in Fig. 4 have the same shape within experimental error. The curve taken at 728°K. shows less curvature in the zero-field region, interpreted to mean the presence of space-charge effects. In the zero-field region, the observed curves fall considerably below the theoretical curve. The experimental curves are so rounded in the region of zero field that determination of zero field is difficult. "Zero field" was therefore arbitrarily determined from the intersection of the line of slope  $-\epsilon/k$  and the "saturation" emission current. The dot-dash line through these intersections shows that the contact potential difference (C.P.D.) is shifting in a fairly regular manner in this case. The other dot-dash line is the result of assuming that the C.P.D. always equals that obtained for 649°K. Other data obtained yielded curves similar to those in Fig. 4, but the changes in C.P.D. for some of these curves are more erratic. This behavior may possibly be the result of an unclean anode. The anode is certainly not clean tantalum, as the C.P.D. is always less than 1.5 volts. The "tails" in the retarding potential region for the curves in Fig. 4 taken at the three highest temperatures are as yet unexplained, but are believed to be an experimental anomaly.

3.2. Thermionic Emission in Accelerating Fields. An electron leaving the surface of an emitter is subjected to a certain force,  $F(z)$ , tending to prevent its escape. For zero applied field, a "zero-field" work function  $\phi_0$  is defined by the equation:

$$\epsilon\phi_0 = \int_0^{\infty} F(z)dz \quad (6)$$

where  $z = 0$  at the "surface" of the emitter. If a field of  $E_a$  volts/cm is applied, the work function is decreased, as the electron is aided by the field, and need only reach the "critical distance"  $z_c$  in order to escape. The work function  $\phi$  is given by:

$$\epsilon\phi = \int_0^{z_c} [F(z) - \epsilon E_a] dz = \epsilon\phi_0 - \int_{z_c}^{\infty} F(z)dz - \int_0^{z_c} \epsilon E_a dz \quad (7)$$

where  $z_0$  is defined by the relation:

$$F(z_c) = eE_a \quad (8)$$

If one assumes that the force function  $F(z) = e^2/4z^2$ , the "image" force, there results from Eqs. (6), (7) and (8) the relation:

$$\varphi = \varphi_0 - \sqrt{eE_a} \quad (9)$$

if we take  $E_a$  as the field at the cathode, a very good approximation since for any appreciable field,  $z_c$  is very small (say  $10^{-2}$  cm or less).

If we assume that the current behaves according to the Richardson-Dushman equation:

$$J = AT^2 \exp(-e\varphi/kt) \quad (10)$$

where  $J = I/(\text{emitting area})$  amp/cm<sup>2</sup>, and that the "constant"  $A$  is not a function of applied field, we have

$$I = I_0 \exp(eE_a/kt) \quad (11)$$

where  $I_0$  is the current at zero field. This is the well-known Schottky relation.

In Fig. 5 are Schottky plots of the thermionic currents at various temperatures. The lines are neither straight over their entire length, nor do the slopes satisfy Eq. (11). The ratio of the observed slope to the theoretical Schottky slope is given in Table I. Note that the slopes deviate

TABLE I.

Temperature	Observed Slope/Schottky Slope	
464°K	17.85	at low fields
	9.25	at high fields
535°K	16.1	at low fields
	8.05	at high fields
600°K	15.5	at low fields
	8.97	at high fields
619°K	14.7	at low fields

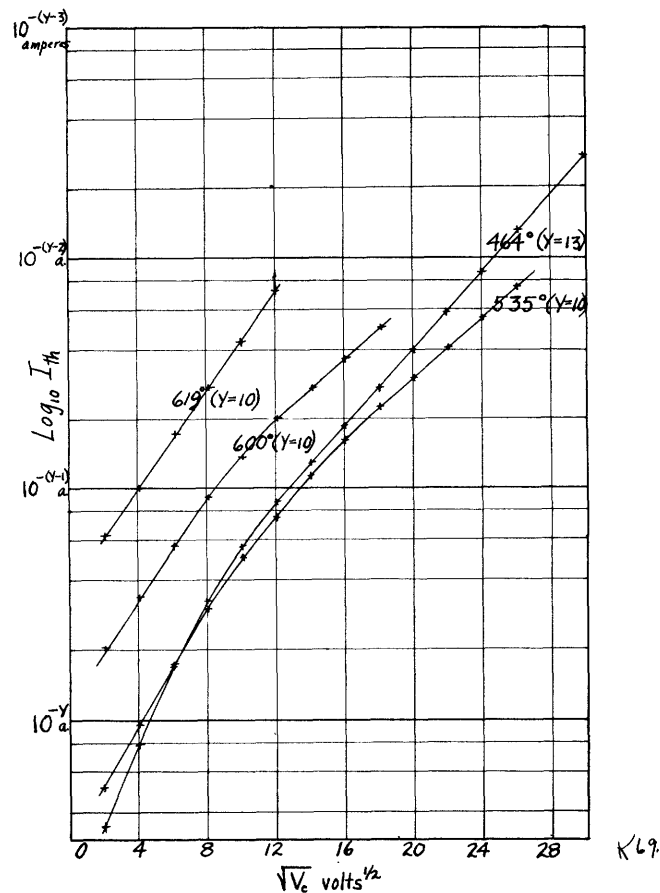


Fig. 5. Schottky plots.

most from the Schottky relation at the lowest temperatures. This fact would make it seem improbable that poor "saturation" for oxide cathodes is due to interstices in the oxide coating where "space charge" could accumulate.

The deviations from the Schottky behavior may be attributed to one of two things. Either (1) the force function  $F(z)$  does not have the form of an image force, or (2) the field  $E_a$  effective at the cathode is not that computed by assuming the cathode to be a "smooth" cylinder. Other data obtained suggest that alternative (1) may be correct, although (2) is not entirely ruled out.

Thermionic emission as a function of temperature is usually plotted on the assumption that Eq. (10) gives the correct temperature variation. Richardson plots are shown in Fig. 6. The plots are straight within experimental error over the considerable temperature range measured. The measurements indicate that  $\phi_{th}$  drops over a tenth of a volt between "zero field" (approximately) and a field of about 110 volts/cm (collector voltage  $V_c = 22\frac{1}{2}$  volts). Equation (9) would give a decrease in  $\phi_{th}$  of only 0.004 volt, too small to be observed experimentally. The "A" factor in Eq. (10) also decreases to about half its value at zero field.

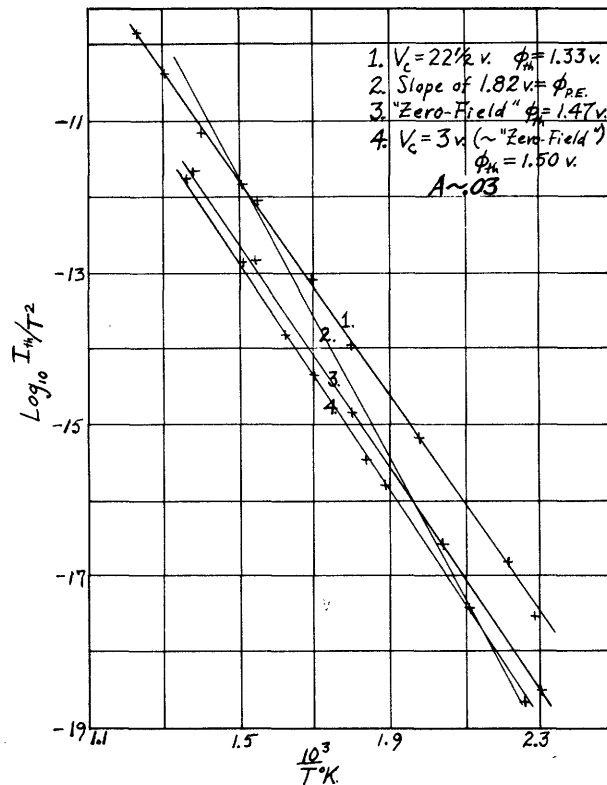


Fig. 6. Richardson plots.

Curve No. 2 in Fig. 6 has a slope corresponding to the "zero field"  $\phi_{P.E.}$ . If  $\phi_{th} = \phi_{P.E.}$  and if the temperature measured as  $400^\circ\text{K}$  is assumed to be correct, the temperature at  $800^\circ\text{K}$  would have to be different from that measured by over 100 degrees. A systematic error in temperature scale of some 20 degrees might be admissible, but a 100-degree error seems highly improbable.

Fowler's equation (1) for thermionic emission from a semi-conductor indicates that the thermionic emission should vary with temperature in accordance with this equation rather than Eq. (10). The plots of Fig. 6 give  $A \approx .03 \text{ amp/cm}^2$  at zero field which is a rather low value. A low value for  $A$  could be the result of electron reflection ( $D < 1$ ), or of an effective emitting area which is less than the geometrical area for smooth-cylinder geometry, or of a smaller  $n_p$  than is usually supposed, or of a positive temperature coefficient for the work function.

**3.3. Coating Conductivity Measurements.** If current is drawn through the oxide coating by the application of a collector voltage, there will be a potential drop occurring in the coating. If the probe assumes the potential of the coating at the location of the probe, one expects that as the "tube current" (current through the coating) increases from zero, the

probe will assume a potential more and more positive with respect to the base metal (nickel sleeve).

In Fig. 7 are shown the  $E_{\text{probe}} - I_{\text{tube}}$  characteristics obtained. Conductivity variation with temperature is so rapid that different vertical

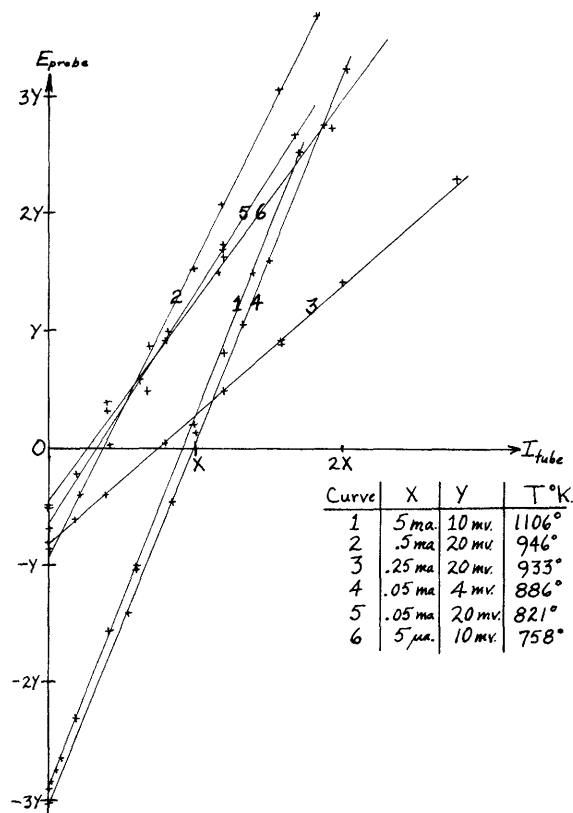


Fig. 7. Probe voltage vs. tube current.

and horizontal scales are used to include all the data in one plot. The slopes are a measure of the resistance of the coating between core and probe, the coating being considered as a "slab" of conductor of a thickness equal to the core-probe separation. The currents drawn were not sufficiently large to produce observable  $I^2R$  heating of the coating. At zero current, the probe voltage is negative rather than zero. This negative potential is believed to be a thermal emf. Becker and Sears<sup>9</sup> demonstrated that this was so by showing that a similar core-oxide-probe system behaved like a source of emf with an internal resistance equal to the coating resistance. As tube current increases from zero, the potential of the probe rises linearly, in accordance with Ohm's Law.

The probe-coating-core system may be considered as two essentially perfect electrical conductors (the core and the probe) embedded in a medium of poor conductivity (the coating). Thus if a potential difference  $E_p$  exists between the probe and the core, a current  $I_p$  should flow in accordance



with Ohm's Law. To a good approximation, the probe-coating-core system may be considered as a conducting cylinder of radius  $r$  immersed in a semi-infinite dielectric, distant  $d$  from an infinite plane conductor. For such a geometry,

$$\sigma = \frac{\cosh^{-1}(d/r)}{2\pi \mathcal{R} L_p} \quad (12)$$

where  $\mathcal{R} = E_p/I_p$  and  $L_p$  is the length of the probe embedded in the coating.

In Fig. 8 are shown some of the experimental results. It is apparent immediately that Ohm's Law is not valid over a wide range of voltages. In addition the curves showed time changes. One might expect difficulties due to polarization effects, the formation of dendrites, etc.

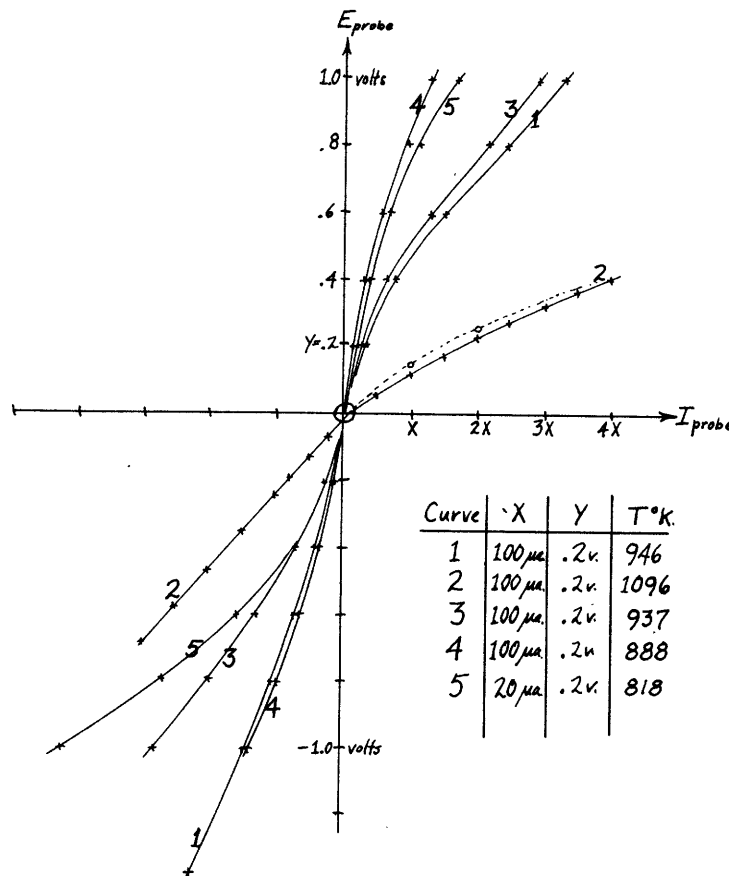


Fig. 8. Probe voltage vs. probe current.

Such characteristics as those of Fig. 8 have been investigated by several experimenters and show more or less erratic behavior. For the purpose of calculating a coating conductivity, it is reasonable to suppose that the resistance  $\mathcal{R} = E_p/I_p$  resulting as  $E_p$  and  $I_p$  approach zero would most nearly correspond to a true coating resistance. Accordingly the asymptotic slope

at the origin was taken to be the resistance  $R$  and the coating conductivity  $\sigma$  calculated from Eq. (12).

In Fig. 9 are shown data of coating conductivity as a function of temperature. The crosses are the data obtained from the plots of Fig. 7,

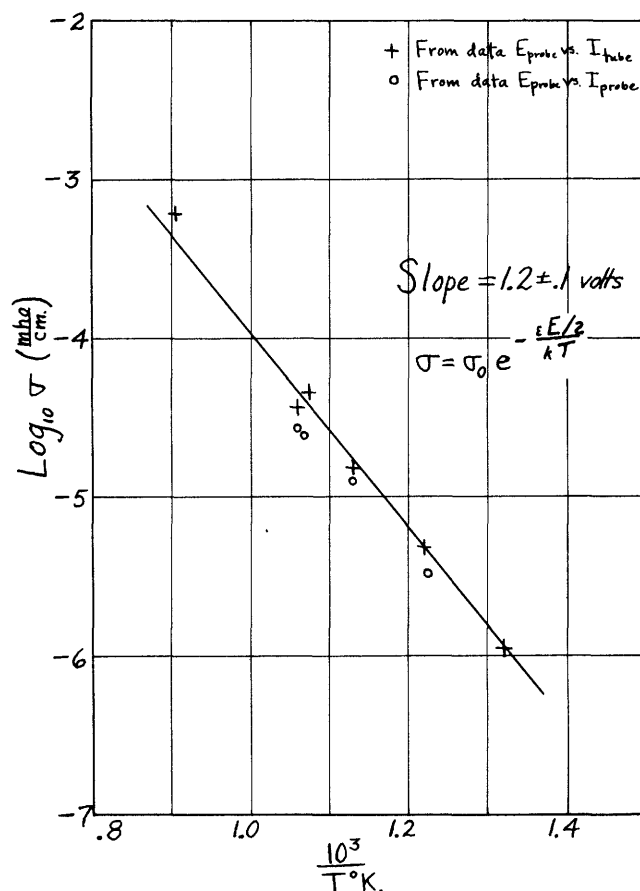


Fig. 9. Coating conductivity as a function of temperature.

and the circles are data from Fig. 8. The two different methods of computing  $\sigma$  agree rather well, and in particular the slopes of the lines through the two sets of data are very nearly the same.

The slope is, of course, the quantity of most interest, since by the simple semi-conductor theory, this slope determines the energy gap  $E$  between the impurity levels and the bottom of the conduction band in the oxide coating, if we consider this coating as a semi-conductor. From the data in Fig. 9, energy gap  $E \cong 2.4 \pm .2$  volts for this particular cathode.

**3.4. Photoelectric Emission.** One would not expect the photoelectric currents due to monochromatic radiation from a semi-conductor to fit a Fowler plot. Brown's work<sup>11</sup> showed that the currents from oxide cathodes did

nevertheless fit a Fowler plot over a limited frequency range, and this result is verified in this research.

In Fig. 10 are shown Fowler plots resulting for various collection voltages. As the field at the cathode increases,  $\phi_{p.E.}$  decreases. The data

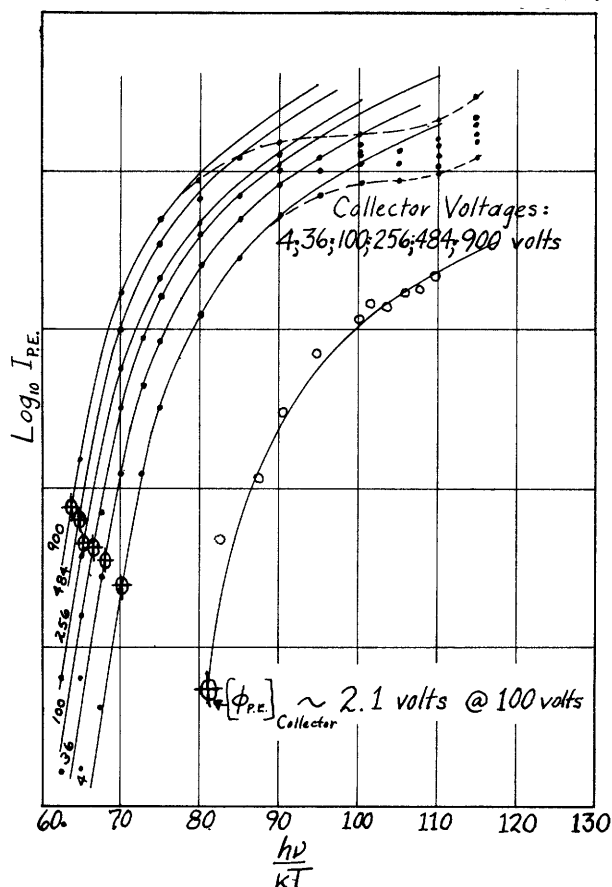


Fig. 10. Fowler plots at room temperature.

obtained from Fig. 10 are plotted in Fig. 11. An approximate extrapolation

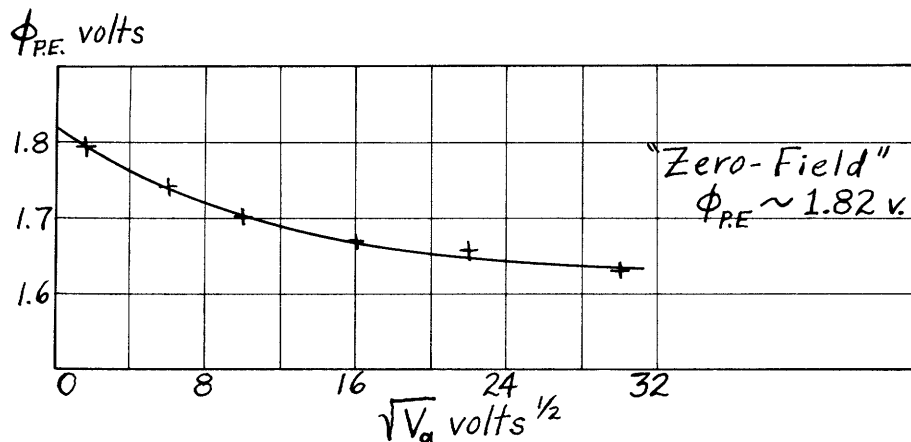


Fig. 11. Variation of photoelectric work functions with the square root of the applied voltage.

to "zero field" gives  $\phi_{p.E.} = 1.82$  volts at zero field.

Figure 10 also shows a single Fowler plot for the collector which indicates a collector work function of about 2.1 volts. As the cathode obstructed the anode, it was difficult to illuminate the anode, so that these data are quite uncertain. The value 2.1 volts is, however, quite reasonable for a surface of barium on tantalum. The C.P.D. of about 1.4 volts does not equal the difference in work functions of anode and cathode, namely (2.1 - 1.5) volts. This can be explained if we assume "patchy" surfaces on the anode and/or the cathode.

In Fig. 12 are shown Fowler plots taken for two different cathode temperatures. The usual plot of  $\log(I/T^2)$  vs.  $(h\nu/kT)$  results in a negative temperature coefficient for  $\phi_{p.E.}$  of about  $3 \times 10^{-4}$  volt/degree. If one plots  $\log(I/T^3)$  vs.  $(h\nu/kT)$  as did Brown,<sup>11</sup> this temperature coefficient becomes almost zero.

The Fowler plots experimentally obtained show deviations from the theoretical Fowler line (the solid lines in Figs. 10 and 12). Thus for all temperatures measured, the experimental points fall quite closely on the theoretical Fowler line for a range in  $(h\nu/kT)$  of about 20, but fall below

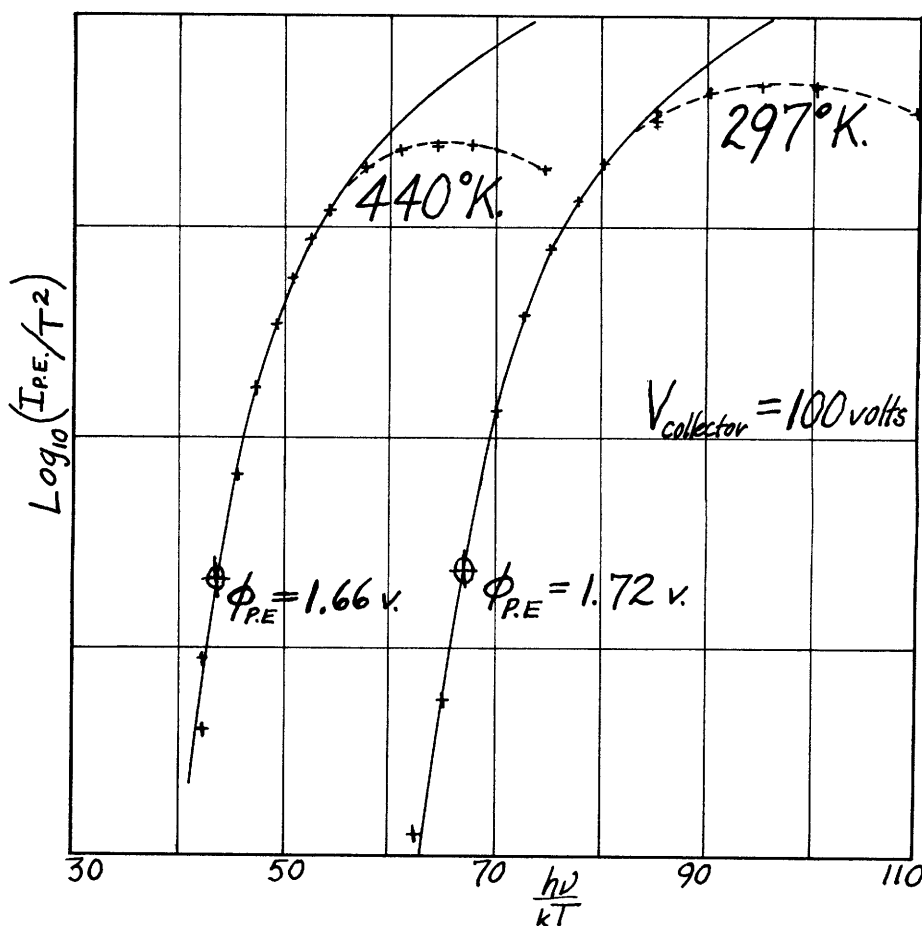


Fig. 12. Fowler plots for two different cathode temperatures.

the line as the frequency becomes higher. Such behavior has been observed for metals<sup>12,13</sup>, and may perhaps be ascribed to a failure of Fowler's simple assumptions at frequencies too far removed from the threshold.

It might be doubted that a Fowler plot for oxide cathode data gives the true  $\phi_{p.e.}$ , especially as the  $\phi_{p.e.}$  so obtained is about 0.15 volt lower than that obtained by the method employed by Nishibori, Kawamura, and Hirano.<sup>10</sup> As a check on the  $\phi_{p.e.}$  determined from Fowler plots, photoelectric currents due to monochromatic illumination were measured in retarding fields. Currents became quite small and difficult to measure in some cases, but at certain wavelengths reasonable accuracy was obtained. The results of some of these measurements are shown in Fig. 13. This

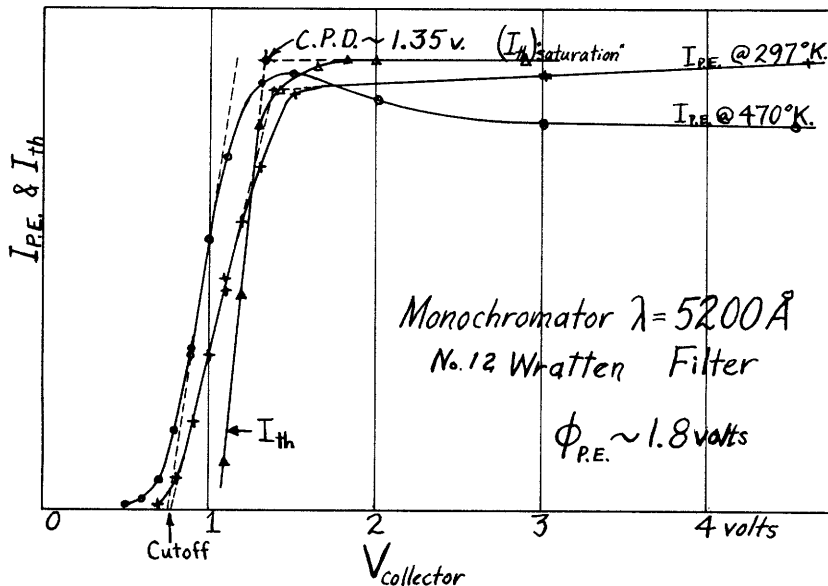
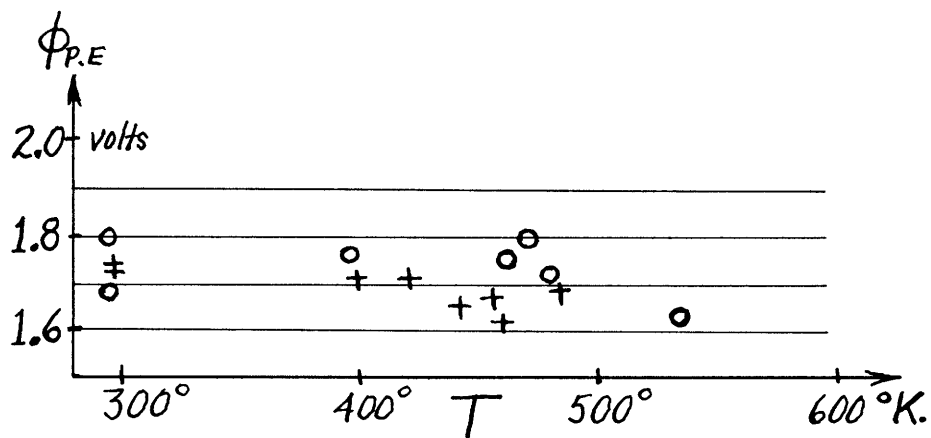


Fig. 13. Currents in retarding fields.

figure shows how the C.P.D. and the "cutoff" can be approximately obtained. Since the wavelength of the illumination is known,  $\phi_{p.e.}$  is determined. The C.P.D. and cutoff determined in this way are somewhat uncertain, but indicate that  $\phi_{p.e.} = 1.8 \pm .1$  volt. The values of  $\phi_{p.e.}$  so determined certainly seem closer to the Fowler plot values, than to those obtained by plotting  $I_{p.e.}$  vs.  $h\nu/kT$  in the manner suggested by Nishibori, Kawamura, and Hirano.<sup>10</sup> In Fig. 14 are given values of  $\phi_{p.e.}$  determined by the procedure shown in Fig. 13, and by means of Fowler plots. Agreement is satisfactory, if one takes account of the drop in  $\phi_{p.e.}$  with applied voltage as shown in Fig. 11.

In Fig. 15 is shown the result of plotting log of the photoelectric current vs. square root of collection voltage (a "Schottky plot") for three different wavelengths of illumination. For a wavelength near the threshold, saturation is very poor, and is still not obtained for a field at the cathode of almost 5000 volts/cm ( $\sqrt{V} = 30 \text{ volts}^{\frac{1}{2}}$ ). Saturation is much



+ Data from Fowler Plots,  $V_c = 100$  v.

o Data from  $I_{P.E.}$  vs  $V$  Plots

Fig. 14. Variation of photoelectric work function with cathode temperature.

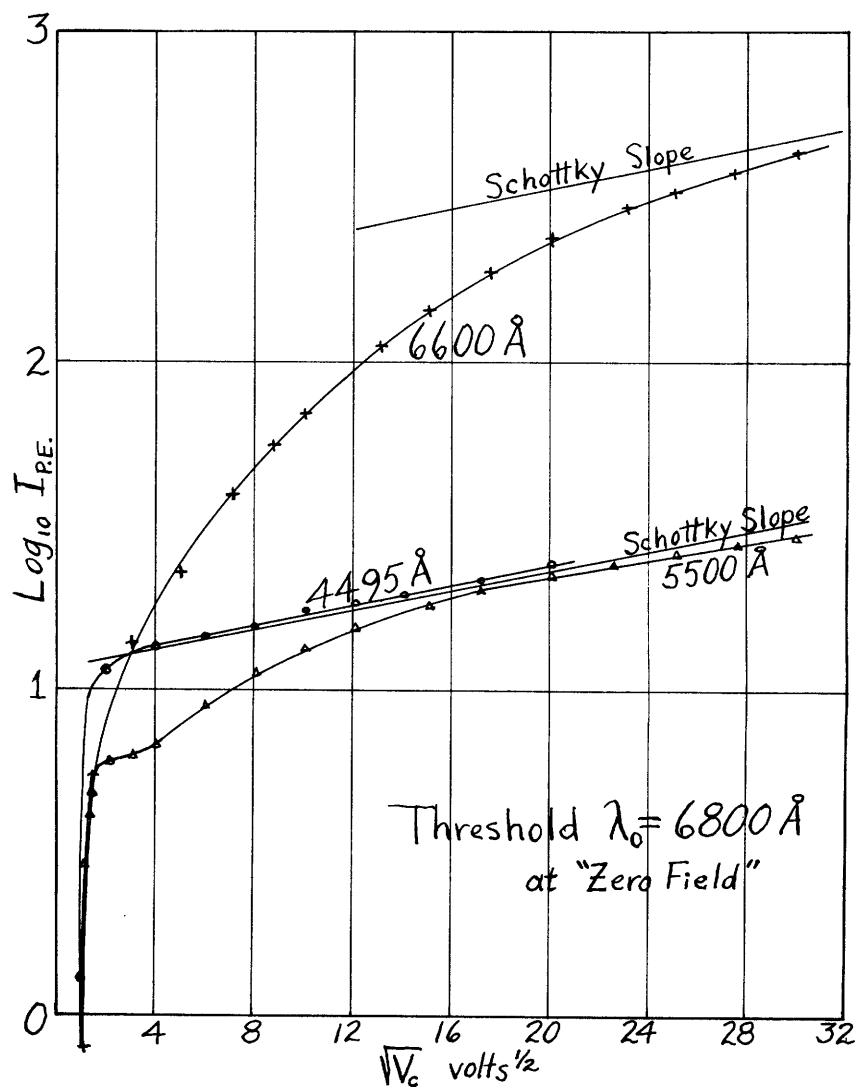


Fig. 15 Schottky plots for photoelectric currents at different wavelengths.

better for wavelengths far removed from the threshold. The slope of the experimental curves approaches closely that of the theoretical Schottky slope if the applied field is sufficiently great.

A search of the literature was made to try to find experimental curves showing a behavior similar to that shown in Fig. 15. Suhrmann<sup>14</sup> obtained curves for various thicknesses of alkali metals deposited on a base metal which showed poorer and poorer saturation as the thickness of the layers decreased, and as the illuminating wavelength approached in value the threshold wavelength. Ives<sup>15</sup> reported a similar behavior for thin films of alkali metals. Brady and Jacobsmeier<sup>16</sup> observed that "saturation" was poorer for thinner films of sodium on aluminum. Huxford<sup>17</sup> obtained for oxide cathodes results qualitatively similar to those of Fig. 15 (using red and green filters).

What the surfaces reported on above have in common is their "patchy" nature. That is to say, different areas of the surface have different work functions. It is felt the assumption of a patchy surface for the oxide cathode explains several observed phenomena, so that the next section will be devoted to a more detailed discussion of patch phenomena.

3.5. Patch Effects. The theory of patches was proposed many years ago by Langmuir in an attempt to explain the poor saturation of thermionic currents from thoriated tungsten. It is physically reasonable to expect that any polycrystalline electron emitter would consist of areas whose dimensions and work functions differ.

Various patch theories have been proposed, making different assumptions as to the shape of the patches, and the means of summing the emission currents from the patch surface. The behavior to be expected of patchy emission surfaces is discussed at some length by Becker,<sup>18</sup> Nottingham,<sup>19</sup> Linford,<sup>20</sup> and others.

A correlation between observed behavior and that to be expected from patch theory is possible by plotting the "surface field"  $E_s$  as a function of distance  $z$  from the emitting surface. This surface field  $E_s$  is the sum of the patch field  $E_p$  and the image field  $E_i$ , and is the force acting on an electron in the  $z$ -direction as it leaves the surface of the emitter, for zero applied field.

The surface field  $E_s$  equals the applied field  $E_a$  at the critical distance  $z_c$ . Differentiating Eq. (7) with respect to field  $E$  gives

$$d\phi/dE_a = -z_c \quad (13)$$

to a good approximation. Hence by knowing the variation of work function

with applied field, the surface field  $E_s$  as a function of distance  $z$  from the cathode is obtained.

The data plotted in Fig. 11 allow a determination of  $d\phi_{p.E.}/dE_a$ . In Fig. 16, the circles represent  $E_s$  as a function of  $z$  on a plot of  $\log E_s$  vs.  $\log z$  as determined from  $d\phi_{p.E.}/dE_a$ . The areas of the circles are meant

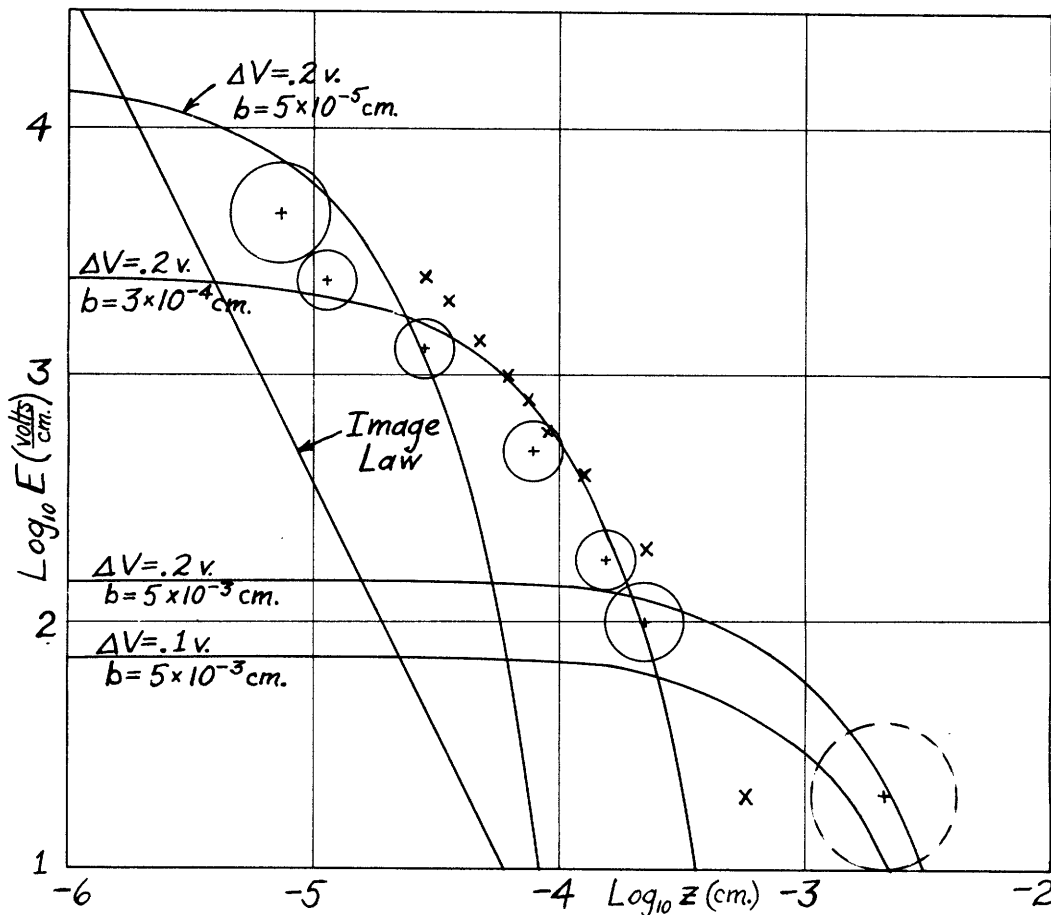


Fig. 16. Electric fields as functions of the distance from the cathode.

to indicate roughly the estimated error in the determination of  $d\phi_{p.E.}/dE_a$ . The variation of  $\phi_{p.E.}$  with field at small fields is the most uncertain, as indicated by the dotted circle.

Thermionic data can also be used to determine  $E_s$  as a function of  $z$ , but more approximations are necessary. If we assume that  $I_{th}$  is given by Eq. (10), and also assume that  $A \neq f(E_a)$ , then we have:

$$d(\log I)/dE_a = d/dE_a \left\{ -1/kT \int_0^{z_c} [F(z) - \epsilon E_a] dz \right\} = \epsilon z_c / kT \quad (14)$$



by using Eq. (7). At distance  $z_c$ ,  $E_s = E_a$  as before, so that  $E_s$  as  $f(z)$  is determined from the slope of a plot of  $\log I_{th}$  vs.  $E_a$  (field at the cathode). In Fig. 16, the crosses are obtained by using the "Schottky" curve in Fig. 5 for 535°K. The other "Schottky" data give points in the same general region on Fig. 16.

The procedure discussed above has uncertainties. The field  $E_a$  may not be that calculated for a smooth - cylinder geometry. Also it is probably not true that  $A \neq f(E_a)$ , although it is likely that the variation of  $\phi_{th}$  with field produces much more change in  $I_{th}$  than does the variation of  $A$  with field. Perhaps some justification for plotting data in this way is that the computed points fall in about the same region in Fig. 16, and that these data can be accounted for by the assumption of patches of reasonable dimensions.

The curved lines in Fig. 16 represent a first approximation to the low work function patch fields for the "checkerboard" patches proposed by Compton and Langmuir, as corrected by Linford.<sup>20</sup> Square patches  $b$  cm on a side are assumed, each patch differing from its neighbor in work function by  $\Delta V$ . The field acting on an electron leaving the surface is:

$$E_s = E_p + E_1 = (8\sqrt{2} \Delta V / \pi b) \exp(-\sqrt{2}\pi z/b) + e^2/4z^2. \quad (15)$$

Different values of  $\Delta V$  and  $b$  give different patch fields, as the curved lines of Fig. 16 show. Most of the data is accounted for by assuming patches approximately  $3 \times 10^{-4}$  cm on a side differing in work function by about .2 volt. The dimensions and work function differences are both reasonable. One would not expect patches of one size only and one work function difference only, so that the values,  $b = 3 \times 10^{-4}$  cm and  $\Delta V = .2$  volt, represent a kind of average for the emitting surface.

Aside from the correlation of data indicated by Fig. 16, other experimentally observed behavior of the oxide cathode can be explained from patch theory. Indeed, some of the behavior is difficult to explain in any other way. Thus the behavior of  $I_{p.e.}$  in accelerating fields illustrated in Fig. 15 has a ready explanation by patch theory. Low energy photons, represented by light of  $\lambda = 6600\text{\AA}$ , extract electrons from low work function areas only. Patch theory shows that the low work function barrier is lowered by a large amount (order of tenths of volts) as the applied field increases. Hence current from these areas would increase rapidly with applied field as observed. High energy photons, represented by light of  $\lambda = 4495\text{\AA}$  in Fig. 15, extract electrons from the entire cathode area, so that the change in current with applied field results from an average for all the patches. The high work function patch barrier is lowered by an

amount less than that for an image field barrier. The net result for this cathode is that the observed "Schottky" slope for  $\lambda = 4495\text{\AA}$  is almost equal to the theoretical Schottky slope for an image barrier. Photons of intermediate energy get electrons from both areas, but the emission from low work function patches finally predominates at high fields. Hence the shape of the curve for  $\lambda = 5500\text{\AA}$  in Fig. 15 can be accounted for by adding two curves resembling those for  $\lambda = 6600\text{\AA}$  and  $\lambda = 4495\text{\AA}$ . This accounts for the inflection point observed in the curve for  $\lambda = 5500\text{\AA}$ .

The large change in  $\phi_{p.e.}$  with applied field (almost .2 volt as the field was increased from 0 to 5000 volts/cm) is of course accounted for by the presence of patches. Apparently  $\phi_{th}$  also decreases with applied field, though accuracy of measurement is poorer for the Richardson plots. Also the "A" factor of Eq. (12) decreases from about .03 at zero field to about half this value for  $E \approx 110$  volts/cm ( $V_c = 22\frac{1}{2}$  volts). A decrease in A due to a decrease in the "area" of the lowest work function areas as the field increases is to be expected from patch theory.

The data in Table I, for the ratio of observed slope to theoretical Schottky slope for thermionic currents would be expected to behave in this manner according to the patch theory worked out by Becker.<sup>18</sup> That is, this ratio should become slightly greater as temperature decreases.

A possible objection to patch theory is that at sufficiently low fields, the observed slope should equal the theoretical Schottky slope. An attempt was made to determine whether or not this objection is valid. In Fig. 17 are shown Schottky plots at low fields, the "accelerating field" being corrected for the estimated C.P.D. It is difficult to work in this region, since "zero-field" is hard to define or measure. The plots in Fig. 17 seem at least to indicate that the observed slope does indeed equal the theoretical slope for a limited range of voltages. Figure 17 is presented as being merely suggestive, not conclusive.

Work done on other composite surfaces indicates that patches on the emitting surface explain much of the observed behavior. The work of Nichols<sup>21</sup> on single crystals of tungsten shows that different crystal faces differ in work function by a few tenths of a volt. Thermionic and photoelectric data for various composite surfaces have been plotted in the manner shown in Fig. 16, and these data fall in about the same region, as plots presented by Nottingham<sup>19</sup> and Linford<sup>20</sup> show. The patches so determined are about  $10^{-3}$  to  $10^{-5}$  cm "square", alternate patches differing in work function by a few tenths of a volt.

3.6. Model of the Oxide Cathode. The original purpose of this investigation was to determine  $\phi_{th}$ ,  $\phi_{p.e.}$ , and the temperature variation of  $\sigma$ . Referring to Fig. 1, the energy gap E was measured to be about  $2 \times 1.2 = 2.4$  volts. Since

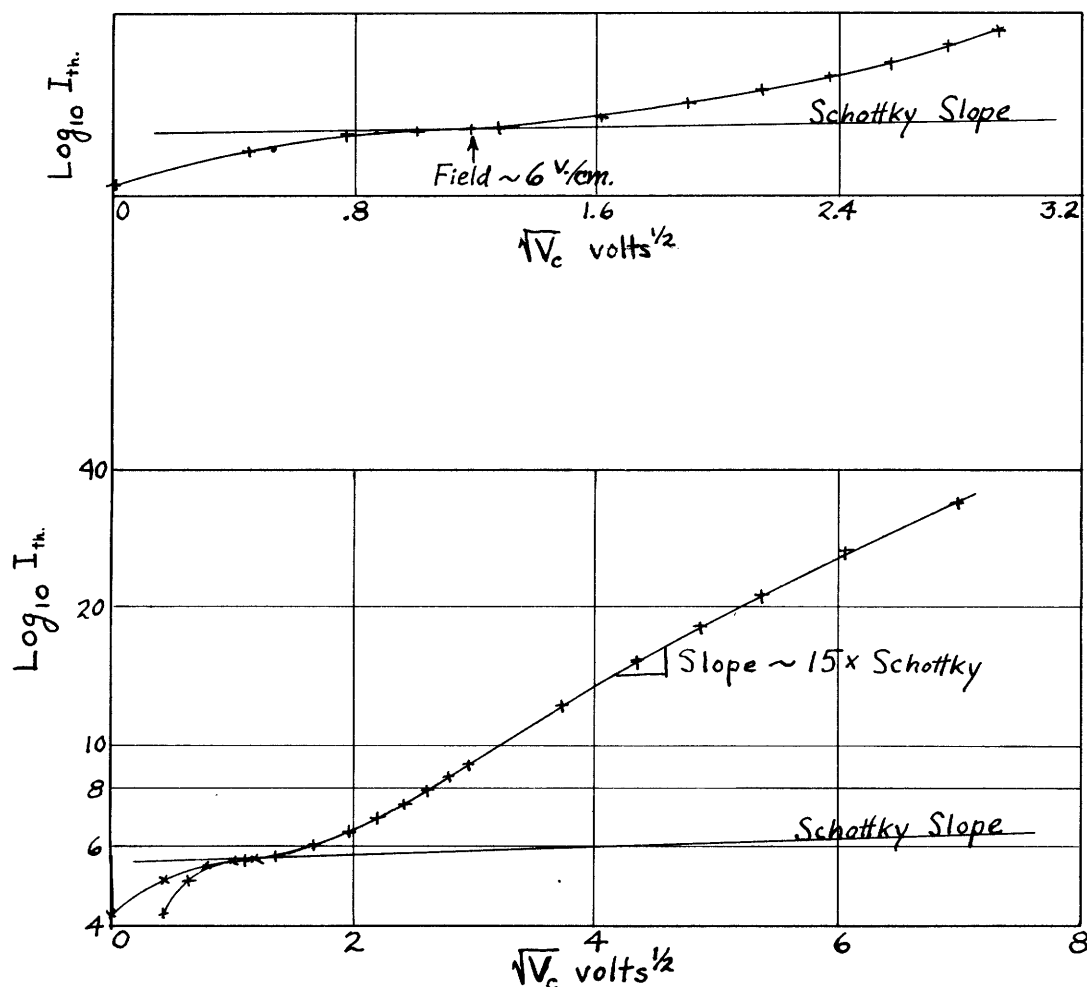


Fig. 17. Schottky plots at low fields.

Richardson plots at "zero field" indicated  $\phi_{th} = 1.5$  volts, and since  $E/2 = 1.2$  volts, the "electron affinity"  $V$  may be taken to be  $1.5 - 1.2 = .3$  volt. This value of  $V$  is in reasonable agreement with those obtained by Nishibori, Kawamura, and Hirano<sup>10</sup>. Outside of their work, the only estimate of  $V$  known to the author is that reported by Vick<sup>3</sup> based on the work of Wright. Wright estimates that  $V$  is less than 0.5 volt.

If surface states played no appreciable part in photoelectric emission, or if these states were non-existent, we should have  $\phi_{p.e.} = E + V$ , assuming the photoelectrons came from the "bound" impurity levels. However,  $\phi_{p.e.}$  was measured to be only about 1.8 volts, not  $E + V \cong 2.4 + .3 = 2.7$  volts. One interpretation of the experimental results obtained is that the photoelectrons come from occupied surface levels having higher energy than the impurity levels in the oxide interior.

One might expect the onset of a "volume photoelectric effect" at about  $4600 \text{ \AA}$ , since

$$\lambda \text{ \AA} = hc/e(V + E) = 12,400/(2.7 \text{ volts}) = 4600 \text{ \AA}.$$

Such an effect would probably be small, as most of the photoelectrons would come from the surface, those in the interior losing energy in the lattice. Certainly no drastic increase in photoelectric current at  $\lambda \sim 4600 \text{ \AA}$  was observed.

There is no justification from the data obtained for the assumption that  $\phi_{p.E.} = V + E$ , as Nishibori, Kawamura, and Hirano<sup>10</sup> have claimed. For the relations (3) to be true, the experimental errors would have to be much greater than what they are estimated to be. This result is really not surprising when one considers that physically there is every reason to suppose that "surface states" do exist.

The photoelectric currents behave in many respects, though not in all respects, like those from metals. Thus the fit of the data to a Fowler plot is remarkably good near the threshold, and Fermi "tails" are observed. Certainly no marked "resonances" occur, as one would expect for electrons emitted from discrete energy levels.

The measurements used to determine energy gaps are not beyond criticism. Thus it has been suggested that in measuring the temperature variation of  $\sigma$  by means of a probe, one is in fact measuring thermionic emission as it varies with temperature. This criticism seems a bit far fetched, however, as there is little in the behavior to suggest thermionic emission, and the measured values of  $E/2$  and  $\phi_{th}$  differ by .3 volt.

The cathode used in these measurements is not the most active attainable, but is representative of some on which measurements have been taken. If we gauge its activity by thermionic work function, the work function is about 1.3 or 1.4 volts, not the "zero-field" value of 1.5 volts. This difference of .1 to .2 volt the writer believes due to decrease in  $\phi_{th}$  with applied field, and probably few values reported in the literature are really "zero-field" values. The value of  $E$  determined is on the high side. The data of Nishibori, Kawamura, and Hirano<sup>10</sup> indicate that a high  $E$  goes with a high  $\phi_{th}$ . The  $\phi_{p.E.}$  checks fairly closely with that of Reference 10, but is .3 to .7 volt higher than those of Huxford<sup>17</sup> or Brown.<sup>11</sup> Activity differences may account for some of the discrepancy.

Acknowledgement. The author wishes to express his thanks to Professor Wayne B. Nottingham and his group for many stimulating discussions concerning the results of this research. Thanks are due also to many members and technicians of the Research Laboratory of Electronics for assistance and advice in the construction of experimental tubes.

## BIBLIOGRAPHY

1. A. Fineman and A. S. Eisenstein, J. App. Phys., 17, 663 (1946).
2. W. E. Mutter, Phys. Rev., 72, 531A (1947).
3. F. A. Vick, Nature, 160, 725 (1947).
4. R. H. Fowler, "Statistical Mechanics", Cambridge Univ. Press, 1936.
5. F. Seitz, "Modern Theory of Solids", McGraw-Hill, 1940.
6. H. Y. Fan, J. App. Phys. 14, 552 (1943).
7. J. P. Blewett, J. App. Phys., 10, 668 (1939).
8. G. E. Moore and H. W. Allison, J. App. Phys. 12, 431 (1941).
9. J. A. Becker and R. W. Sears, Phys. Rev. 38, 2193 (1931).
10. E. Nishibori, H. Kawamura, and K. Hirano, Proc. Phys. Math. Soc., Japan, 22, 378 (1940); 23, 37 (1941).
11. B. B. Brown, M.I.T. Sc. D. Thesis, "An Investigation of Certain Electrical Properties of Oxide-Coated Cathodes", 1942; unpublished.
12. L. Apker, E. Taft, and J. Dickey, Phys. Rev., 73, 46 (1948).
13. R. J. Cashman and E. Bassoe, Phys. Rev., 55, 63 (1939).
14. R. Suhrmann, Naturwiss., 16, 336 (1928).
15. H. E. Ives, Astrophys. J., 60, 209 (1924).
16. J. J. Brady and V. P. Jacobsmeier, Phys. Rev., 49, 670 (1936).
17. W. S. Huxford, Phys. Rev., 38, 379 (1931).
18. J. A. Becker, Rev. Mod. Phys., 7, 95 (1935).
19. W. B. Nottingham, Phys. Rev., 49, 78 (1936).
20. L. B. Linford, Rev. Mod. Phys. 5, 34 (1933).
21. M. H. Nichols, Phys. Rev., 57, 297 (1940).

